AIRFOIL DESIGN FOR SAILPLANES AND ULTRALIGHT AIRCRAFT

by J. Reneaux, A.M. Rodde, J.J. Thibert, ONERA, Chatillon, France

Presented at the XXV OSTIV Congress, Saint Auban, France

SUMMARY

ONERA has been involved over the last twenty years in different studies related to sailplanes and the objective of this paper is to present the main contributions in airfoil design.

The OAP airfoil family was designed to obtain a very high lift-to-drag ratio mainly in thermal flight. These airfoils were used to define the wings of Pegasus and Marianne sailplanes produced by Societe Nouvelle Centrair. More recently, airfoils with flaps have been designed with thickness-to-chord ratio between 13% and 18%.

Two airfoils devoted to ultralight aircraft and general aviation are also presented.

For these applications, the paper describes the flow phenomena which have to be considered for the design (transition of the boundary layer, separation bubbles, stall behaviour), the design process and the performances of the different airfoils.

1. INTRODUCTION

ONERA has many years of experience in research on airfoil design for various applications including civil transport aircraft wings, helicopter blades and propellers. During the last twenty years, this know-how has also been applied to different studies related to low speed application and the main objective of this paper is to present the contribution to sailplane airfoil design.

2. AERODYNAMICS OF SAILPLANES

The flight conditions encountered by sailplanes include climb in thermals at low flight speeds and high lift coefficients, and interthermal cross-country flight at higher speeds. The performance in cross-country conditions weighs strongly on the global efficiency of modern sailplanes, which is why a code has been developed to predict sailplane aerodynamic characteristics in these conditions. This code allows the lift-to-drag ratio of a sailplane to be estimated using the computed 2D airfoil characteristics and the sailplane geometry. As an example, Figure 1 presents the comparison of measured and computed polars of the Pegasus sailplane for a flight mass of 330 kg. Good correlation between prediction and measurements shows that this approach can be used to estimate the sensitivity of the sailplane polar to an airfoil modification.

The interest of using water ballast in soaring flight is also underlined by Figure 1, as an increase of the sailplane mass improves the performance at high speed. In addition, this approach provides data on the drag breakdown of sail-

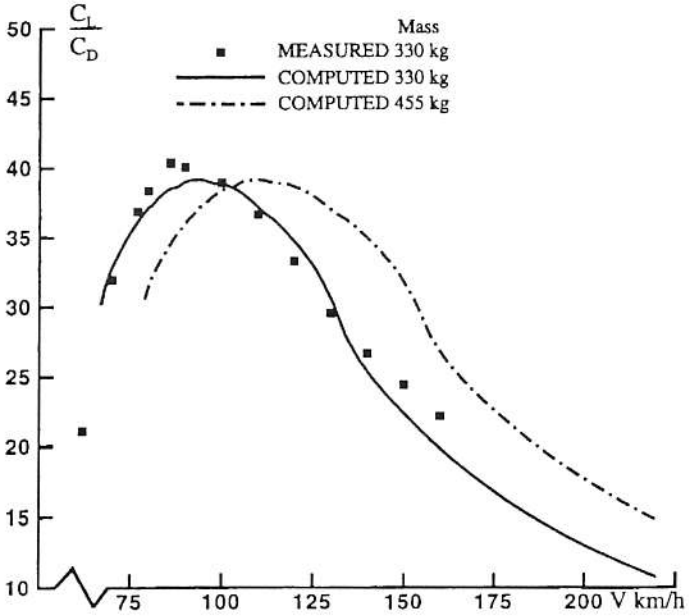

Figure 1. Measured and computed polars of the Pegase sailplane.

planes and the Figure 2 shows the computed contribution of the wing to the total drag.

At 100 km/h, the wing induced drag and the wing viscous drag have the same relative value while at high speed the wing viscous drag has the greatest importance.

Whatever the flight conditions, the wing drag represents at least 75% of the total drag which shows the interest of using efficient airfoils.

3. DESIGN METHOD

Airfoil performance is determined using 2D strong coupling codes [1], [2] which compute the viscous flow around airfoils indicating the extent of laminar flow, the presence of laminar separation bubbles and the regions of turbulent

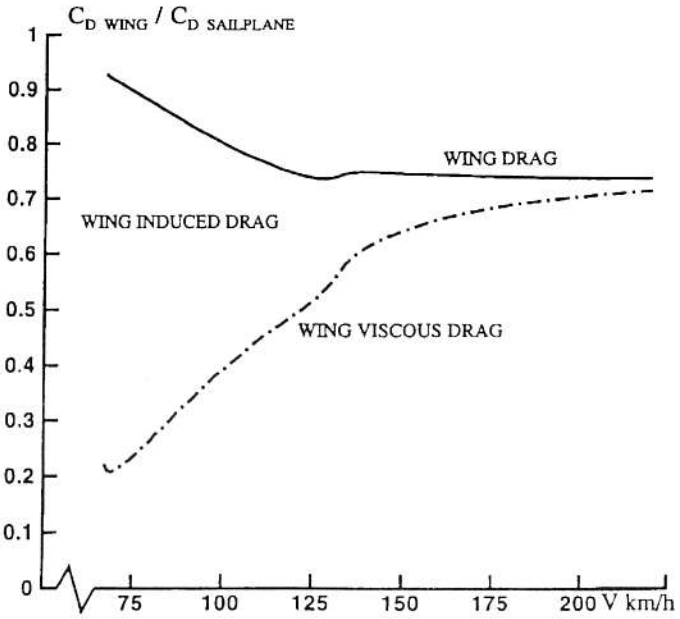

Figure 2. Drag breakdown of the Pegase sailplane.

separation. Figure 3 shows the computed drag polar and the pressure distributions of the FX61-147 airfoil at a Reynolds number of 1.4 10^6. The low drag coefficient is obtained with a great extent of laminar flow on both sides of the airfoil, the transition of the boundary layer being caused by laminar separation bubbles. At high lift coefficient the transition moves upstream on the upper surface while a loss of laminar flow appears on the lower surface for low lift coefficients. The sailplane airfoil design requires then, great attention to these transition movements and to the extent of the laminar separation bubbles [3].

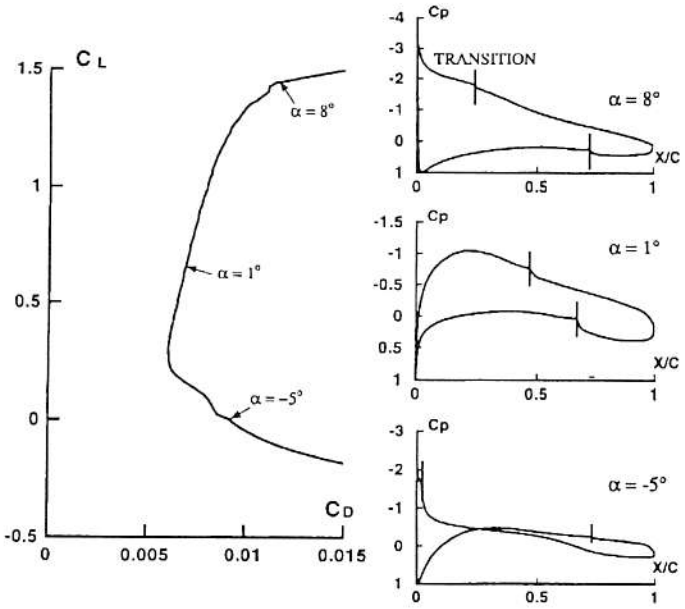

Figure 3. Aerodynamic characteristics of the FX61-147 airfoil. M=0.12, Re=1.4 10^6.

The importance of the viscous effects on the pressure distribution is shown in Figure 4. The difference in lift coefficient is about 13.5% in these conditions.

The sailplanes airfoils are defined with a multipoint design as the climbing in thermals and the cross-country flight require good characteristics at different lift coefficients. Both inverse codes and numerical optimization methods are currently used at ONERA for airfoil design. The inverse methods allow an airfoil corresponding to a prescribed pressure distribution to be obtained while the numerical optimization method [4] combines a flow solver with a constrained minimization algorithm. The numerical optimization method offers the possibilities to consider global coefficients of the airfoil, to impose geometric constraints and to take into account several design points whereas these specifications cannot be taken into account by the inverse methods.

Generally at ONERA, the airfoil is defined in a first step using the numerical optimization method to obtain a global compromise between the different flight conditions and is modified in a second step with an inverse code to adjust the pressure gradients in order to obtain specific characteristics related to transition location and stall behaviour.

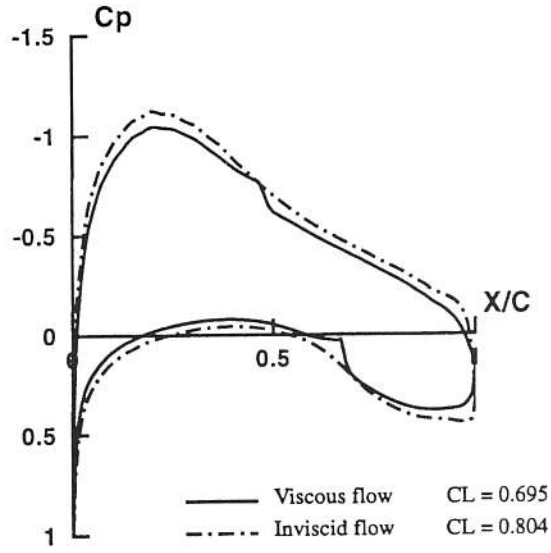

Figure 4. The influence of viscous effects on the pressure distribution of the FX61-147 airfoil. M=0.12, α=1°, Re=1 .4 10^6.

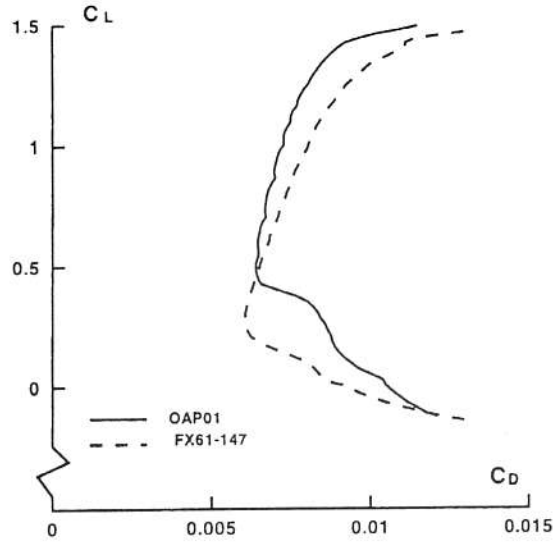

Figure 5. Computed drag polars of the OAP01 and FX61-147 airfoils. M=0.12, Re=1.4 10^6.

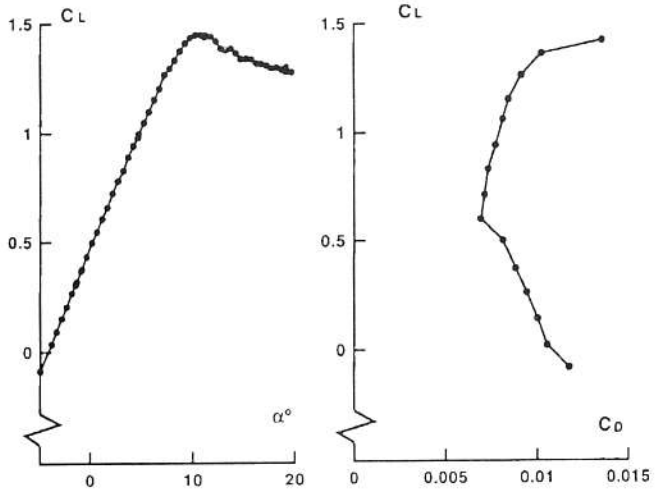

Figure 6. Measured polars of the OAP01 airfoil. M=0.12, Re= 1.4 10^6.

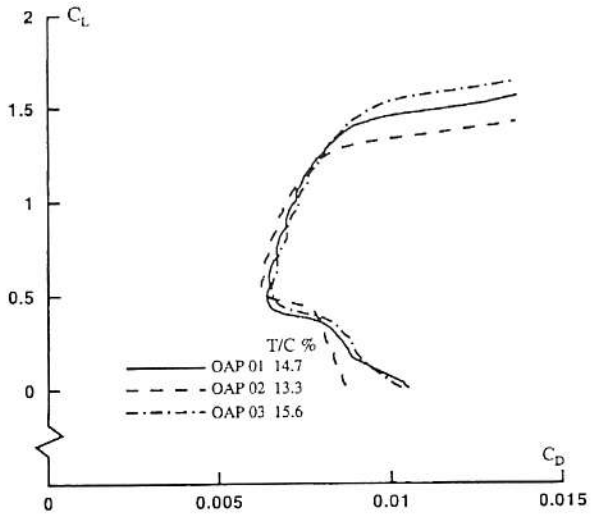

Figure 7. Computed drag polars of the OAP airfoil family. M=0.12, Re=1.4 10^6.

4. AIRFOILS FOR THE STANDARD CLASS

In 1981, the Centrair company launched the Pegasus with the objective of offering a Standard Class sailplane which exhibits good performance in competition whilst keeping safe flight behaviour adapted to beginners. Since then, about 600 sailplanes of this type have been produced and sold.

ONERA designed the wing airfoils of the Pegasus, named OAP01, OAP02 and OAP03 with the objective of obtaining:

- Very good performance in climb conditions;
- Progressive stall behaviour;
- Maximum lift coefficient insensitive to insect contamination.

The computed aerodynamic characteristics of the OAP01 airfoil have been compared to those of the FX61-147 airfoil (which was at that time considered as a reference) in Figure 5. Both airfoils have a thickness-to-chord ratio close to 14.7%. The OAP01 airfoil has a greater lift-to-drag ratio for the lift range $0.4 < C_L < C_{Lmax}$ and the absolute value of the moment coefficient at 25% of the chord is reduced by about 20%.

The performance of the OAP01 airfoil which was measured in the S10 wind tunnel of the CEAT in Toulouse is presented in Figure 6. It shows that for a Reynolds number of 1.4 10^6, the maximum lift coefficient of this airfoil reaches 1.45 and that the loss of lift beyond C_{Lmax} appears progressively.

The performances of the OAP02 and OAP03 airfoils, having thickness to chord ratios of 13.3% and 15.6% respectively, are compared to the OAP01 characteristics in Figure 7. The increase of the thickness-to-chord ratio allows the laminar bucket to be maintained for a larger lift coefficient range but leads to a rise of the minimum drag.

This OAP airfoil family has also been used to generate the wing of the Marianne, a two-seater high-performance sailplane.

For some Pegasus evolutions, the airfoil family, named OAPC, was derived from the previous one in order to increase the performance in interthermal flights at low lift coefficients. The OAPO1 and OAPC01 airfoil characteristics are compared in Figure 8. The laminar bucket of the OAPC01 airfoil is shifted to lower lift coefficients and has a slightly greater extension in lift coefficient. The two families whose main differences are the leading edge geometries (from 0% to 20% of the chord) can be used to adapt the sailplane characteristics to specific conditions.

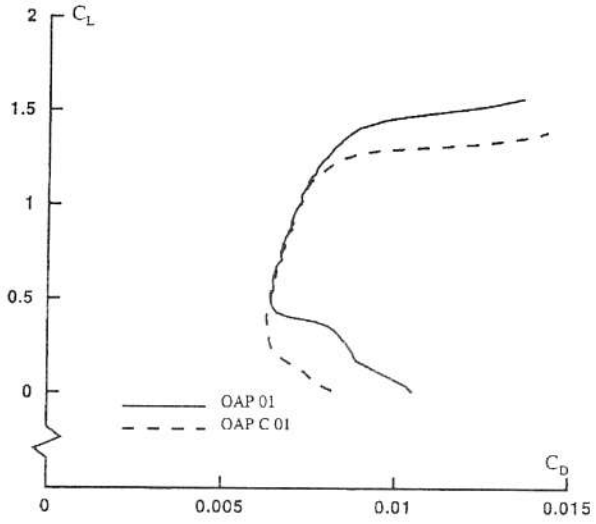

Figure 8. Comparison of computed characteristics of OAPO1 and OAPC01 airfoils. M=0.12, Re=1.4 10^6.

5. AIRFOILS WITH FLAPS

For the 15-Meter Class and the Open Class, flaps are used to adapt the camber of the wing to flight conditions: the flight between the thermals is usually carried out at a low flap setting (zero or slightly negative) while the flight in the thermals requires a high lift coefficient and positive flap settings of about 10° depending on the airfoil. Three airfoils, named OAPV13, OAPV15 and OAPV18 were designed for a thickness-to-chord ratio of 13%, 15% and 18% respectively and for a flap chord of 15%.

As an example, the Figure 9 presents the pressure distributions of the OAPV13 airfoil for three flap settings δ=-10°, δ=0° and δ=10° at an angle of attack of 1°. The laminar flow extent obtained on the OAPV13 airfoil with zero flap setting is about 80% of the chord on the lower surface and 60% of the chord on the upper surface ensuring a very low drag coefficient. Changing the flap deflection has a strong effect on the lift coefficient (from 0.09 to 1.13). Some pressure peak appears at the hinge position on the lower surface for negative flap deflections and on the upper surface for positive ones. Some interesting discussions of the effects of the sailplane flap can also be found in [5].

The performance of this airfoil was measured in the S10 wind tunnel of the CEAT. The use of the flap increases the maximum lift coefficient from 1.4 to 1.53 when the flap setting changes from zero to 10°. Figure 10 compares the computations and the experimental results for the C_L (α)

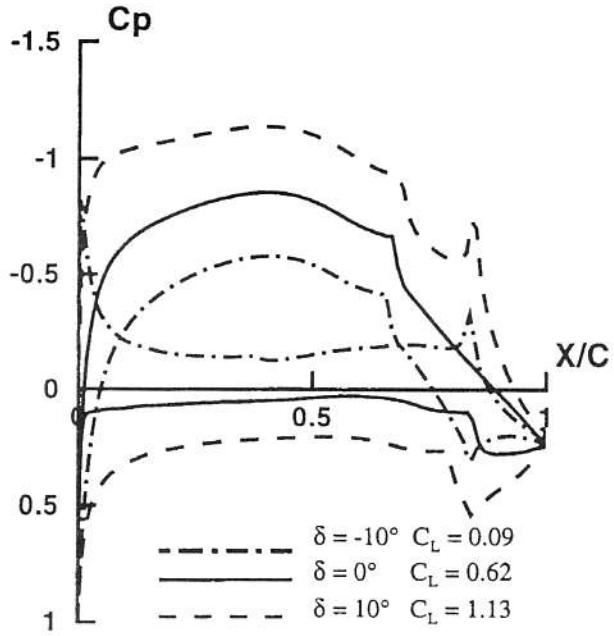

Figure 9. Computed pressure distributions of the OAPV13 airfoil. M=0.12, α=1°, Re=1.4 10^6.

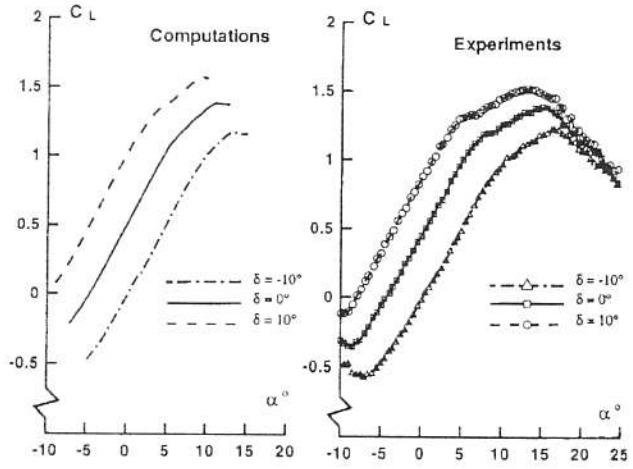

Figure 10. Computed and measured characteristics of the OAPV13 airfoil. M=0.12, Re=1.4 10^6.

curves. The effects of the flap setting is correctly predicted in the linear region and close to the maximum lift, but the stall characteristics can only be determined by wind tunnel tests.

The laminar bucket is also strongly modified by the flap setting as shown in Figure 11: it is shifted by $\Delta C_L \approx 0.3$ for a modification of flap setting of 10°.

Based on these polars, the code described in section 2 can also be used to predict the modification in the sailplane polar with the flap setting. The sailplane performance is presented in Figure 12 for the three flap settings δ= -10°, δ=0° and δ=10°. In thermals, the sailplane typically climbs with positive setting. The maximum lift-to-drag ratio is obtained between 80 km/h and 125 km/h with zero flap setting while the greatest performance in interthermal flight at high speed is obtained with negative flap setting.

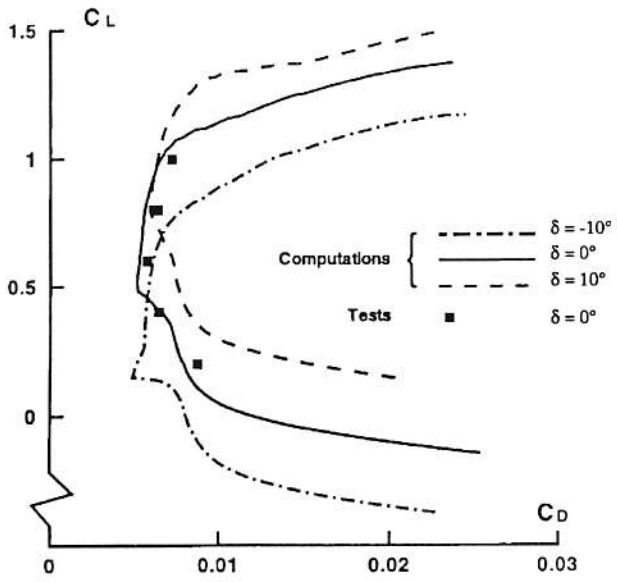

Figure 11. Influence of the flap setting on the polar of the OAPV13 airfoil. M=0.12, Re= 1.4 10^6.

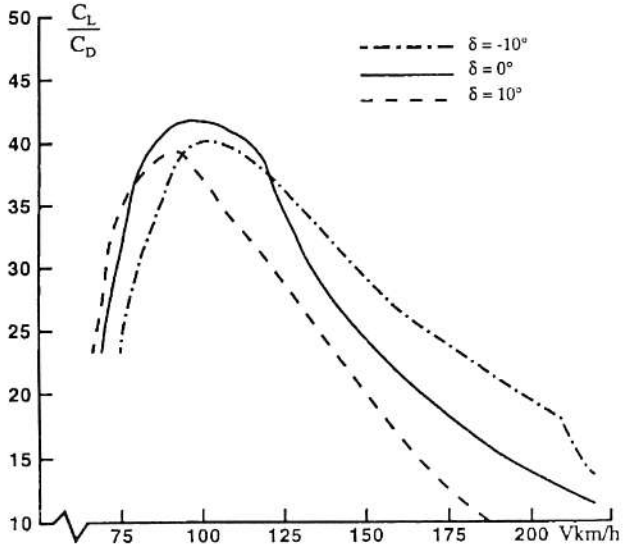

Figure 12. Influence of the flap deflection on the sailplane performance.

This approach shows that it is possible to optimize numerically the flap settings of a sailplane.

Figure 13 presents the computed drag polars of the three airfoils which constitute the OAPV family. The increase of the thickness-to-chord ratio leads to the rise of the minimum drag coefficient but allows the laminar bucket to be maintained for a greater range of lift coefficients.

As the same tendencies have been noticed for the Standard Class airfoils, the Figure 14 summarizes the influence of the thickness-to-chord ratio for the OAP, OAPC and OAPV families. The increase of the drag coefficient is about 1.6 counts for an additional 1% in the thickness-to-chord ratio that is to say about 2.7% of the airfoil drag. These results can be used as basic data to study the compromise between the aerodynamic and the structural characteristics for the optimization of the sailplane configuration.

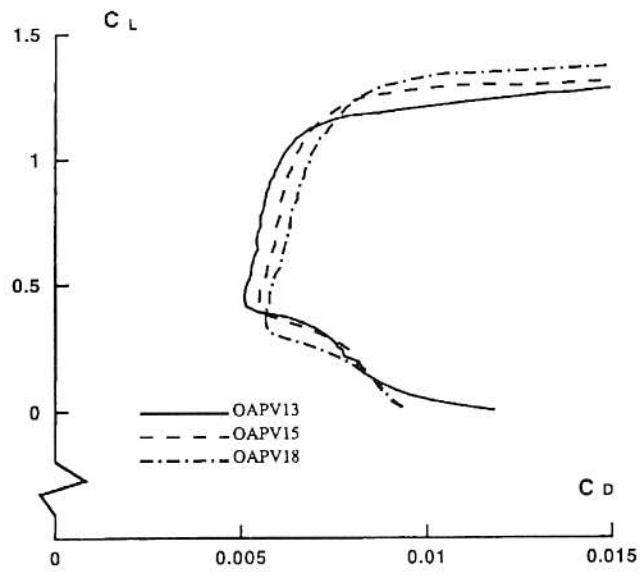

Figure13. Computed drag polars of the OAPV airfoil family. M=0.12, Re=1.4 10^6.

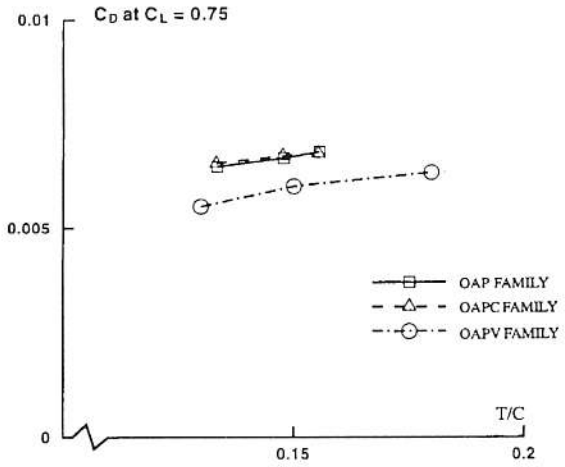

Figure 14 . Influence of the thickness-to-chord ratio on the drag coefficient at C_L=0.75, M=0.12 and Re=1.4 10^6.

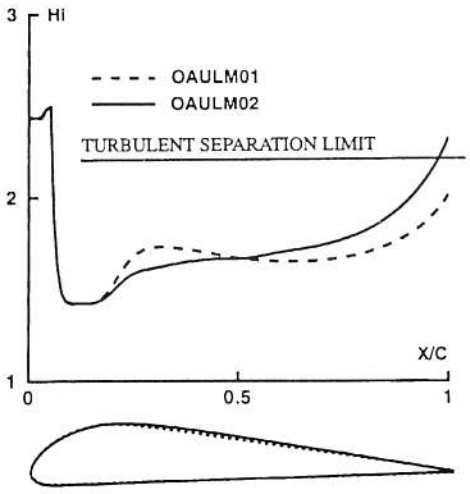

Figure 15. Geometries and computed suction side shape factor of airfoils for ultralight aircraft. M=0.12, C_L=1.65, Re=1.4 10^6, transition triggered at 5%.

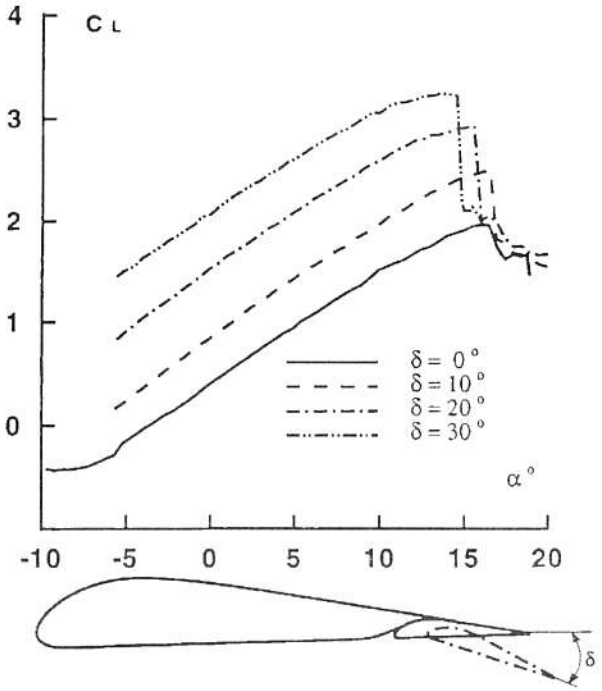

Figure 16. Experimental lift coefficient of the OAULM02 airfoil with a single slotted flap. M=0.12, Re=1 .4 10^6.

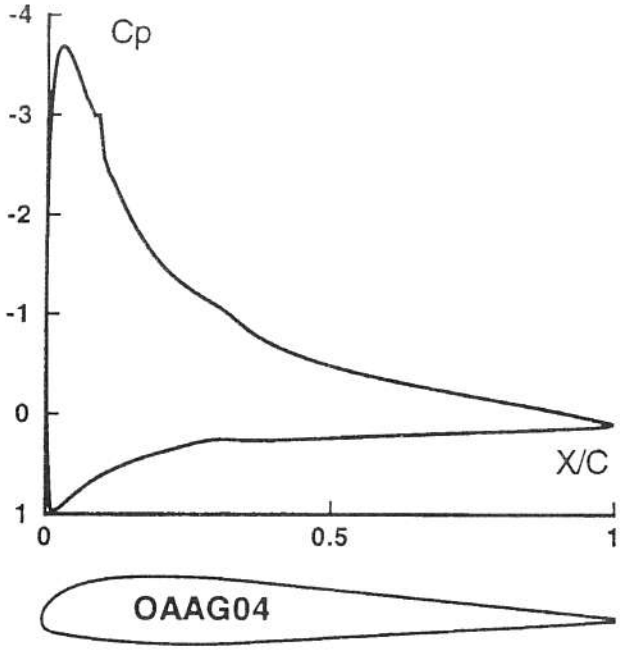

Figure 17. Geometry and computed pressure distribution of the OAAG04 airfoil. M=0.12, C_L=1.2, Re=2 10^6.

6. AIRFOILS FOR ULTRALIGHT AIRCRAFT AND GENERAL AVIATION

6.1. Airfoil for ultralight aircraft

ONERA also designed airfoils for general aviation aircraft. As far as the ultralight aircraft are concerned, the design specifications are summarized by the following:

- A very high maximum lift coefficient at low Reynolds numbers to fly at very low speed and to make very short landings;
- A smooth stall behaviour due to the relative inexperience of the potential users;
- A pitching moment lower than 0.05 in absolute value to reduce the drag penalty due to the balance of the aircraft;
- A thickness-to-chord ratio of 14% and a flat lower surface to simplify the manufacture.

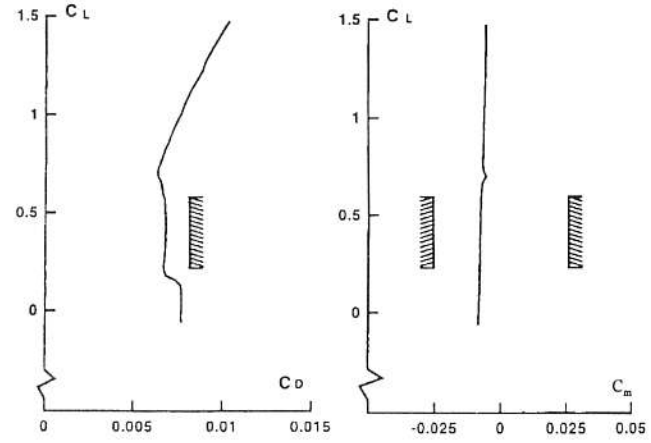

Figure 18. Computed characteristics of the OAAG04 airfoil. M=0.12, Re=4.5 10^6.

A first airfoil was designed and tested in the S10 wind tunnel. The results showed that the aerodynamic characteristics of this airfoil were of interest for the application considered, except that the stall was too steep. To remedy this, the airfoil was modified so that the turbulent separation appears in the trailing edge region and grows progressively. The OAULM02 airfoil is the result of this second design and Figure 15 compares the geometries and the computed boundary layer shape factors along the upper surface of both airfoils. The margin with respect to the turbulent separation limit is small at 30% of the chord for the OAULM01 airfoil while the shape factor of the OAULM02 airfoil grows progressively in the turbulent region.

Following a second test campaign whose results are presented in Figure 16, the airfoil OAULM02 exhibits a very high maximum lift coefficient of 1.96 at a Reynolds number of 1.4 10^6 with the absolute value of the moment coefficient remaining less than 0.05. In addition, it can be equipped with a single slotted flap having a 27% chord length. The Figure 16 shows that in this condition the maximum lift increases from 1.96 to 3.24 for a flap deflection of 30° without a large modification of the stall angle.

This application shows how some specifications related to the airfoil stall can be taken into account despite the inaccuracy of the method enabling the maximum lift coefficient and the type of the stall to be computed directly.

In addition to ultralight aircraft, the OAULM02 airfoil has also been applied, with success, to racing car wings, rigid sails for boats, and paragliders, for which the Reynolds numbers are moderate and close to the design conditions.

6.2 . Airfoil for general aviation

The OAAG04 airfoil of a thickness-to-chord ratio of 12% was designed for general aviation applications. The design specifications are related in this case to the maximum lift

coefficient, the drag and moment coefficients and to geometrical constraints as follows:

- $C_{Lmax} \geq 1.6$ at $Re=2\ 10^6$;
- $CD \leq 0.008$ and $|Cm| \leq 0.025$ for $0.2 \leq C_L \leq 0.6$ at $Re=4.5\ 10^6$;
- Linear shape between 30% of the chord and the trailing edge on both surfaces.

The computed pressure distribution of the OAAG04 airfoil which was designed for this purpose is presented in Figure 17 at a lift coefficient of 1.2. It appears that this airfoil exhibits a low leading edge expansion and a suitable pressure recovery to obtain a high maximum lift coefficient. A C_{Lmax} of 1.75 was measured in the S10 wind tunnel.

Figure 18 presents the computed characteristics of the OAAG04 airfoil in cruise conditions and shows that both design specifications related to drag and moment coefficient have been achieved. In particular, the low drag region of the airfoil has been well adjusted to the desired lift coefficients.

The OAAG04 airfoil has been used to define the wing of the CAPX, which is a two-seater training aircraft.

These two examples shows how specifications related to the drag and to the maximum lift coefficient can be fulfilled and that the problems encountered in general aviation are close to those of the sailplane activities.

7. CONCLUSIONS

ONERA has developed methods for both airfoil design and performance calculation taking into account the viscous phenomena which govern the flow at moderate Reynolds numbers. Several airfoil families were designed for Standard Class sailplanes and for sailplanes with flaps: the first family was successfully applied on Pegase and Marianne wings. Two other airfoils were also designed for ultralight aircraft and general aviation applications.

ACKNOWLEDGMENTS

The authors would like to thank C. Le Tallec and P. Fely, both engineers at ONERA for the valuable discussions related to their experience as sailplane pilots.

REFERENCES

1. Drela, M., Giles, M.B. - ISES; A Two-dimensional Viscous Aerodynamic Design and Analysis Code, AIAA Paper 87-0424, 1987.
2. Le Balleur, J.C. - Strong Matching Method for Computing Transonic Viscous Flows Including Wakes and Separations. Lifting Airfoils, La Recherche Aerospatiale, 1983-3, French and English Editions.
3. Van Ingen, J. L., Boermans, L.M.M. - Research on Laminar Separation Bubbles at Delft University of Technology in Relation to Low Reynolds Number Airfoil Aerodynamics, Conference on low Reynolds Number Airfoil Aerodynamics, UNDAS-CP-77B123, June, 1985.
4. Reneaux, J., Thibert, J.J. - The Use of Numerical Optimization for Airfoil Design, AIAA 85-5026, Colorado Springs, 1985 T.P. ONERA 1985-135.
5. Boermans, L.M.M., Van Garrel, A. - Design and Wind Tunnel Test Results of a Flapped Laminar Flow Airfoil for High-Performance Sailplane Applications, XXIV OSTIV Congress, Omarama, New Zealand, 1995.